

Resonance eigenfunction hypothesis for chaotic systems

Konstantin Clauß,¹ Martin J. Körber,¹ Arnd Bäcker,^{1,2} and Roland Ketzmerick^{1,2}

¹Technische Universität Dresden, Institut für Theoretische Physik and Center for Dynamics, 01062 Dresden, Germany

²Max-Planck-Institut für Physik komplexer Systeme, Nöthnitzer Straße 38, 01187 Dresden, Germany

(Dated: March 8, 2018)

A hypothesis about the average phase-space distribution of resonance eigenfunctions in chaotic systems with escape through an opening is proposed. Eigenfunctions with decay rate γ are described by a classical measure that (i) is conditionally invariant with classical decay rate γ and (ii) is uniformly distributed on sets with the same temporal distance to the quantum resolved chaotic saddle. This explains the localization of fast-decaying resonance eigenfunctions classically. It is found to occur in the phase-space region having the largest distance to the chaotic saddle. We discuss the dependence on the decay rate γ and the semiclassical limit. The hypothesis is numerically demonstrated for the standard map.

PACS numbers: 05.45.Mt, 03.65.Sq, 05.45.Df

Introduction.—Chaotic scattering [1] appears in many fields of physics, such as nuclear reactions [2], microwave resonators [3], acoustics [4] and quantum dots [5]. Another prominent example are optical microcavities [6], where the emission patterns depend on the properties of resonance modes of the cavity. Thus it is of great interest to understand the properties of resonance eigenfunctions. They are expected to be universal for fully chaotic systems. For closed systems the *semiclassical eigenfunction hypothesis* states that eigenfunctions are concentrated on those regions explored by typical classical orbits [7–9]. If the dynamics is ergodic, this is proven by the quantum ergodicity theorem [10–15], showing that almost all eigenfunctions converge to the uniform distribution on the energy shell in phase space [16]. For scattering systems many aspects of resonance eigenfunctions have been studied, e.g. for open billiards [17–21], optical microcavities [22–27], and maps [28–35], however, there exists no analogue to the semiclassical eigenfunction hypothesis, not even for chaotic systems.

The simplest setting are time-discrete maps with chaotic dynamics and escape through an opening. Quantizing the map yields a subunitary propagator whose non-orthogonal, right eigenfunctions have varying decay rates γ . Note that these eigenfunctions extend into the opening for the chosen ordering of escape before the mapping. Surprisingly, there occurs a localization of their average phase-space distribution within the opening. This localization is more prominent for resonance eigenfunctions with large decay rates γ , as visualized for the standard map (introduced below) in Fig. 1 (top). Thus, the following questions arise: What is the origin of this localization? What distinguishes the phase-space region of localization? More generally, is this effect caused by quantum interference (like dynamical localization [36] or scarring due to periodic orbits [37]) or by properties of the classical dynamics?

Before answering these questions, let us briefly introduce the classical and quantum mechanical background.

Classically, for chaotic dynamics of a map with escape almost all points on phase-space Γ will be mapped into the opening Ω eventually and thus escape [38]. Only a set of measure zero does not leave the system under forward and backward iteration. This invariant set usually is a fractal and is called the *chaotic saddle* Γ_s , see Fig. 2(a). Its unstable manifold consists of points

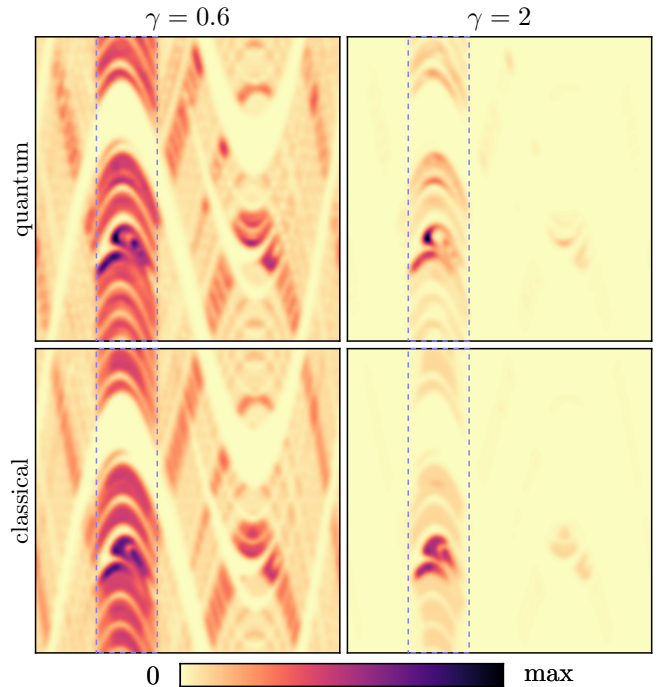


FIG. 1. Average Husimi phase-space distribution of resonance eigenfunctions (top) compared to constructed classical measures μ_γ^h (bottom) with decay rates $\gamma = 0.6$ (left) and $\gamma = 2$ (right) for $h = 1/1000$. Chaotic standard map with $\kappa = 10$ on phase space $\Gamma = [0, 1) \times [0, 1)$ with opening $\Omega = [0.2, 0.4) \times [0, 1)$ (blue dashed line). Colormap with fixed maximum for each γ . Prominent localization for $\gamma = 2$ and overall quantum-classical agreement.

approaching Γ_s under the inverse map and is therefore called the *backward-trapped set* Γ_b , see Fig. 2(b). Generic initial phase-space distributions asymptotically converge to the uniform distribution on Γ_b , the so-called *natural measure* μ_{nat} , with corresponding decay rate γ_{nat} [39–44].

Quantum mechanically, the support of resonance eigenfunctions is given by the backward trapped set Γ_b [28, 30]. Furthermore, long-lived eigenfunctions with decay rates $\gamma \approx \gamma_{\text{nat}}$ are distributed as the natural measure μ_{nat} on phase space [28], which corresponds to the steady-state distribution in the context of optical microcavities [23]. There are a few supersharp resonances with γ significantly smaller than γ_{nat} [45]. Instead, we focus on the large number of shorter-lived eigenfunctions ($\gamma > \gamma_{\text{nat}}$). Their integrated weight on Ω and on each of its preimages (shown in Fig. 2(c)) depends on the decay rate γ [30]. This concept is generalized by so-called conditionally invariant measures [31, 39, 42, 43]. Recently, we suggested a specific conditionally invariant measure proportional to μ_{nat} on the opening Ω , describing classically the weight of eigenfunctions on either side of a partial barrier [35]. None of these results, however, explains the observed localization phenomenon.

In this paper we propose a hypothesis for resonance eigenfunctions in chaotic systems predicting their average phase-space distribution. The hypothesis defines a conditionally invariant measure of the classical system for given decay rate γ and effective Planck's constant h . It gives a classical explanation for the localization of resonance eigenfunctions in those phase-space regions having the largest distance to the chaotic saddle. This is demonstrated in Fig. 1 for the chaotic standard map. We discuss the dependence on γ and h , and briefly speculate about the semiclassical limit.

Resonance eigenfunction hypothesis.—We postulate that in chaotic systems with escape through an opening the average phase-space distribution of resonance eigenfunctions with decay rate γ for effective Planck's constant h is described by a measure that (i) is conditionally invariant with decay rate γ and (ii) is uniformly distributed on sets with the same temporal distance to the h -resolved chaotic saddle.

Combining both properties yields a measure

$$\mu_\gamma^h(A) = \frac{1}{\mathcal{N}} \int_A e^{t_h(x) \cdot (\gamma - \gamma_{\text{nat}})} d\mu_{\text{nat}}(x), \quad (1)$$

for all $A \subset \Gamma$ with normalization constant \mathcal{N} . Here the temporal *saddle distance* $t_h(x) \in \mathbb{R}$ fulfills

$$t_h(M^{-1}(x)) = t_h(x) - 1 \quad (2)$$

for all $x \in \Gamma_b$, i.e. each backward iteration of the map M on Γ_b reduces the saddle distance by one. An important implication of Eq. (1) is that μ_γ^h is enhanced with increasing $\gamma > \gamma_{\text{nat}}$ in those regions of Γ_b having the largest saddle distance, due to the exponential factor.

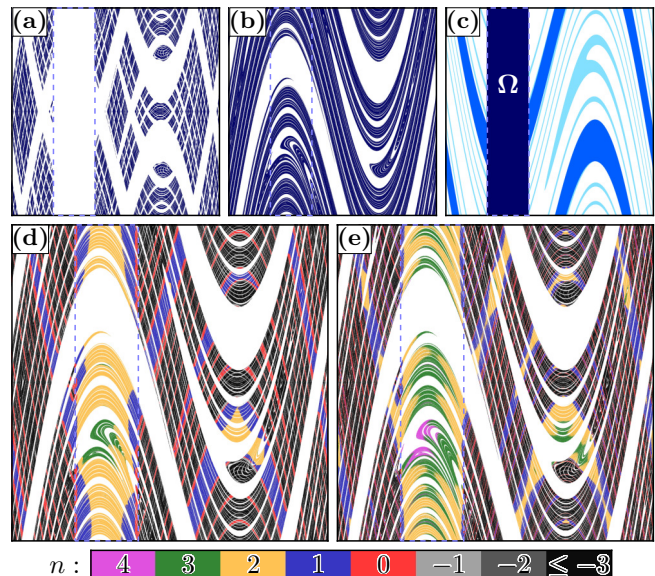


FIG. 2. Classical sets for the considered standard map. (a) Chaotic saddle Γ_s , (b) backward trapped set Γ_b , (c) opening Ω and preimages $M^{-1}(\Omega)$, $M^{-2}(\Omega)$ (from dark to light), (d, e) partition of the backward trapped set Γ_b with colored sets \mathcal{E}_n^h with integer saddle distance $n \leq m_h$ for (d) $h = 1/1000$ with $m_h = 3$ and (e) $h = 1/16000$ with $m_h = 4$. Regions with $n \leq 0$ are within the h -resolved saddle Γ_s^h .

These regions must be in the opening Ω , which is easily shown by contradiction. Thus the hypothesis leads to a classical prediction for the localization of resonance eigenfunctions in chaotic systems.

We will now discuss properties (i) and (ii) in more detail. A measure μ is called conditionally invariant with decay rate γ under a map M with escape through an opening, if it is invariant under time evolution up to an overall decay,

$$\mu(M^{-1}(A)) = e^{-\gamma} \mu(A), \quad (3)$$

for all $A \subset \Gamma$ [39, 42, 43]. Equation (3) states that the set $M^{-1}(A)$, which consists of points that are mapped onto A , has a measure that is smaller by a factor $e^{-\gamma}$ than the measure of A . The support of conditionally invariant measures is the backward trapped set Γ_b . The most important of these measures is the natural measure μ_{nat} with decay rate γ_{nat} [42, 43]. This measure is uniformly distributed on the backward trapped set Γ_b . We stress that for any decay rate γ there are infinitely many different conditionally invariant measures [31, 43]. So far it is unknown, if any of these classical measures corresponds to resonance eigenfunctions with arbitrary decay rates.

Property (ii) selects a specific class of measures which are uniformly distributed on subsets of Γ_b . Uniform distribution with respect to Γ_b (the support of conditionally invariant measures) is equivalent to proportionality to the natural measure, explaining the appearance of μ_{nat} in Eq. (1). In analogy to quantum ergodicity for closed

systems it is reasonable to consider for resonance eigenfunctions a uniform distribution on Γ_s , as classically this is an invariant set with chaotic dynamics. The quantum mechanical uncertainty relation, however, implies a finite phase-space resolution \hbar replacing Γ_s by a quantum resolved saddle Γ_s^h . It is desirable to combine the assumption of uniformity on the saddle, the finite quantum resolution, and conditional invariance. This is achieved by introducing a temporal distance $t_h(x)$ to the quantum resolved saddle Γ_s^h for all $x \in \Gamma_b$ and assuming uniformity on all sets with the same temporal distance. The resulting measures μ_γ^h , Eq. (1), are conditionally invariant according to Eq. (3) as can be shown using Eq. (2).

For the saddle distance $t_h(x)$ we now provide a conceptually and numerically simple implementation. For this we consider as a convenient definition of Γ_s^h a symmetric surrounding of Γ_s , $\Gamma_s^h = \{x \in \Gamma : d(x, \Gamma_s) \leq \sqrt{\hbar/2}\}$, with Euclidean distance d smaller than the width of coherent states. We define an *integer saddle distance* $n \in \mathbb{Z}$ for $x \in \Gamma_b$ as the number of backward steps to enter the \hbar -resolved saddle,

$$t_h(x) = n \Leftrightarrow M^{-n}(x) \in \Gamma_s^h, \quad (4)$$

with $M^{-i}(x) \notin \Gamma_s^h$ for all $i < n$. For points inside of Γ_s^h this leads to $n \leq 0$. Defining $\mathcal{E}_n^h := \{x \in \Gamma_b : t_h(x) = n\}$ as the sets with integer saddle distance n we obtain a partition of Γ_b with $\mathcal{E}_n^h = M^n \mathcal{E}_0^h$. There is a maximal saddle distance m_h , and consequently the regions \mathcal{E}_n^h with $n > m_h$ are empty sets. With this Eq. (1) simplifies to

$$\mu_\gamma^h(A) = \frac{1}{\mathcal{N}} \sum_{n=-\infty}^{m_h} e^{n(\gamma - \gamma_{\text{nat}})} \mu_{\text{nat}}(A \cap \mathcal{E}_n^h), \quad (5)$$

for all $A \subset \Gamma$, which will be applied in the following.

Example system.—Throughout this paper we use the paradigmatic example of the standard map [46] in its symmetric form $(q, p) \mapsto (q + p^*, p^* + v(q + p^*))$ with $p^* = p + v(q)$ and $v(q) = (\kappa/4\pi) \sin(2\pi q)$, considered on the torus $q \in [0, 1)$, $p \in [0, 1)$ with periodic boundary conditions. We consider a kicking strength $\kappa = 10$ to ensure a fully chaotic phase space. The opening is chosen as a vertical strip Ω , such that $q \in [0.2, 0.4]$ and $p \in [0, 1)$, see Fig. 1. Position and size of Ω determine the classical decay rate $\gamma_{\text{nat}} \approx 0.21$ of the natural measure μ_{nat} .

We consider the Floquet quantization U_{cl} [47, 48] of the closed map on a Hilbert space of dimension $1/\hbar$ with effective Planck's constant \hbar . The quantum map is opened as $U = U_{\text{cl}} \cdot (\mathbb{1} - P_\Omega)$ with projector P_Ω on the opening [49]. The eigenvalue problem of this subunitary propagator, $U\psi = \lambda\psi$, leads to eigenvalues with modulus less than unity, $|\lambda|^2 \equiv e^{-\gamma} < 1$. The decay rate γ characterizes the time evolution of the corresponding resonance eigenfunction ψ . There is a broad distribution of decay rates γ [29, 49]. We compute the Husimi phase-space distribution $\mathcal{H}(q, p) = 1/\hbar |\langle q, p | \psi \rangle|^2$ for each eigenfunction

ψ by taking the overlap with symmetric coherent states $|q, p\rangle$ centered at $(q, p) \in \Gamma$.

While Husimi distributions \mathcal{H} of individual resonance eigenfunctions show strong quantum fluctuations, we want to explain their average behavior. Therefore we calculate the average Husimi distribution $\langle \mathcal{H} \rangle_\gamma$, where the average is taken over eigenfunctions from the interval $[\gamma \cdot c, \gamma/c]$ around some γ -value of interest with constant $c = 0.95$. We improve this averaging by increasing the number of contributing Husimi distributions in two ways: First, we vary the Bloch phase $\theta_p \in \{0.04, 0.08, \dots, 0.96\}$ of the quantization U . Secondly, the inverse Planck's constant is varied in $\{0.94, 0.96, 0.98, 1, 1.02, 1.04, 1.06\} \cdot \hbar^{-1}$ for $\hbar = 1/1000$.

Classical measures μ_γ^h are obtained as follows. Using the sprinkler method [38] we approximate the chaotic saddle Γ_s as a point set with more than 10^7 points not leaving the system under ten forward and backward time steps, see Fig. 2(a). Tenfold forward iteration of this set gives an approximation of Γ_b , see Fig. 2(b). The uniform distribution on this point set approximates μ_{nat} which is used in Eq. (5). We partition Γ_b into sets \mathcal{E}_n^h by determining the integer saddle distance n for each $x \in \Gamma_b$, such that $d(M^{-n}(x), \Gamma_s) \leq \sqrt{\hbar/2}$ and $d(M^{-n+1}(x), \Gamma_s) > \sqrt{\hbar/2}$, shown in Figs. 2(d) and (e) for two values of \hbar . Note that the region with maximal saddle distance m_h is similar for both considered \hbar . The saddle distance n varies for points on Γ_b and in particular on the opening Ω for two reasons: the geometric distance along the manifold to the quantum resolved saddle Γ_s^h and the variation of the local stretching, i.e. finite time Lyapunov exponents. In order to construct μ_γ^h , we assign to each $x \in \Gamma_b$ a weight $e^{n(\gamma - \gamma_{\text{nat}})}$ according to the factor in Eq. (5). Integrating these weights over grid cells with chosen resolution 800×800 and normalizing we obtain a phase-space density numerically approximating μ_γ^h . After smoothing this classical measure with a Gaussian of width $\sqrt{\hbar/2}$, i.e. the width of coherent states, it can be compared to the phase-space distribution of eigenfunctions.

Comparison.—In Fig. 1 we show the average phase-space distributions $\langle \mathcal{H} \rangle_\gamma$ for $\gamma = 0.6$ and $\gamma = 2$ for $\hbar = 1/1000$. This is compared to the constructed measures μ_γ^h smoothed with a Gaussian of width $\sqrt{\hbar/2}$. Overall we observe very good agreement concerning the support of the distributions, their weight on the opening Ω , and their localization within Ω .

The Husimi distributions show the following features: First, they are supported by the smoothed backward trapped set. Secondly, one observes that their density on the opening Ω is larger than on its surrounding. The other stripes with larger density (than their surrounding) fall on the preimages $M^{-1}(\Omega)$ and $M^{-2}(\Omega)$, shown in Fig. 2(c). Thirdly and most importantly, the Husimi distributions within Ω are not uniform on Γ_b , but show

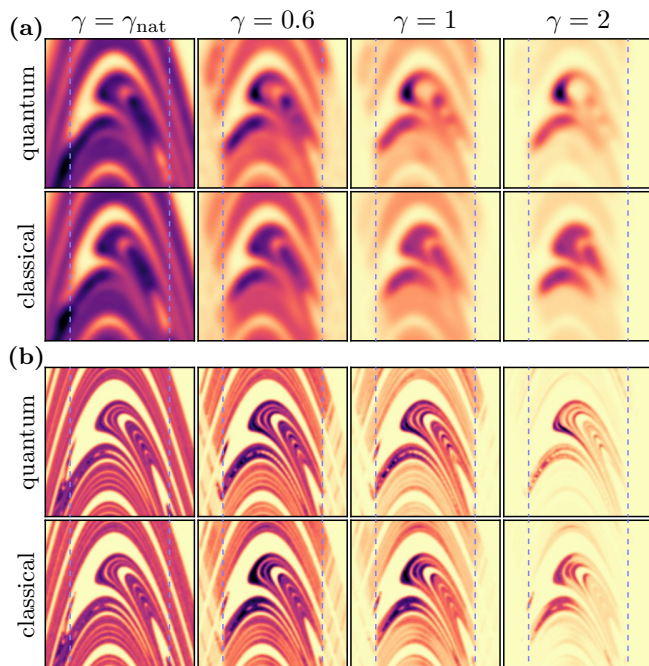


FIG. 3. Average Husimi distribution of resonance eigenfunctions (top) compared to constructed classical measures μ_γ^h (bottom) with $\gamma \in \{\gamma_{\text{nat}}, 0.6, 1, 2\}$ for (a) $h = 1/1000$ and (b) $h = 1/16000$ on phase-space region $[0.15, 0.45] \times [0.15, 0.45]$. Colormap as in Fig. 1, with fixed maximum for each γ in (a) and in (b).

localization, which is stronger for larger γ .

The same three observations hold for the constructed measures μ_γ^h , where they directly follow from properties (i) and (ii). The first two observations are implied by conditional invariance. Note that the integrated weight on Ω increases with γ as $\mu_\gamma^h(\Omega) = 1 - e^{-\gamma}$, which follows from Eq. (3). It also implies for the k -th preimage of the opening $\mu_\gamma^h(M^{-k}(\Omega)) = e^{-k\gamma} \mu_\gamma^h(\Omega)$, which agrees with the quantum mechanical analysis [30]. For the third observation we explicitly need the saddle distance in our classical construction, which follows from property (ii). Those parts of Ω with maximal saddle distance m_h , see Fig. 2(d), show the largest enhancement due to the exponential factor in Eq. (5). Consequently, regions with smaller saddle distance are less enhanced. In conclusion we have found a classical explanation for the localization of resonance eigenfunctions. In particular, this shows that it is not an interference effect.

Dependence on γ .—In Fig. 3(a) we illustrate quantum (top) and classical (bottom) phase-space distributions zoomed into the phase-space region $(q, p) \in [0.15, 0.45] \times [0.15, 0.45]$ for increasing decay rates γ starting with γ_{nat} for $h = 1/1000$. This region is chosen to contain the significant peaks in Ω . As expected, at the natural decay rate γ_{nat} the Husimi distribution is almost perfectly resembled by the (smoothed) natural measure μ_{nat} . Eigenfunctions with larger γ show an increasingly prominent

localization. Classically, this is reproduced using the measures (5). Note that at $\gamma = 2$ also differences between classical and quantum densities can be seen. The main peak is sharper and stronger localized quantum mechanically than for the classical construction. We attribute this to the chosen simplification using an integer saddle distance.

Dependence on h .—Figure 3(b) shows the corresponding sequence of plots for much smaller effective Planck's constant $h = 1/16000$. The eigenfunctions resolve finer structures of the backward trapped set. Again, similarly good agreement between quantum and classical densities is found. In particular one observes stronger density variations on Γ_b in form of arcs, e.g. for $\gamma = 1$. Classically their origin is the increased maximum saddle distance $m_h = 4$ and the finer partition of Γ_b seen in Fig. 2(e) especially in the opening. Furthermore, the sets of maximal saddle distance m_h are similar, see Figs. 2(d) and (e), such that the localization occurs in a similar region in Figs. 3(a) and (b). Again, at $\gamma = 2$ sharper and stronger peaks occur in the quantum distribution than classically.

While numerically it is not possible to go to much smaller values of the effective Planck's constant h , we briefly speculate about the semiclassical limit. Decreasing h gives a smaller surrounding of Γ_s , such that the saddle distance $t_h(x)$ increases for all $x \in \Gamma_b$, including the maximum m_h . If for decreasing h the difference $m_h - t_h(x)$ converges, one can show that the measures μ_γ^h converge towards a family of γ -dependent measures. In this case according to hypothesis a semiclassical convergence of the eigenfunctions is expected.

Discussion.—We have shown that the proposed resonance eigenfunction hypothesis for chaotic systems gives a classical explanation of the quantum mechanically observed localization. The resulting measures μ_γ^h reproduce the average phase-space distribution of resonance eigenfunctions. Small deviations might be improved by more elaborate definitions of Γ_s^h and the saddle distance $t_h(x)$, e.g. by considering in the definition of Γ_s^h the distance along the unstable manifold or by considering continuous saddle distances from a smooth quantum resolved saddle. An application of the hypothesis to time-continuous systems, like open billiards, should be straightforward. A future challenge is the application to optical microcavities, which requires a generalization to partial transmission and reflection.

We are grateful to E. G. Altmann, L. Bunimovich, T. Harayama, E. J. Heller, S. Nonnenmacher, and H. Schomerus for helpful comments and stimulating discussions, and acknowledge financial support through the Deutsche Forschungsgemeinschaft under Grant No. KE 537/5-1.

-
- [1] P. Gaspard: *Quantum Chaotic Scattering*, Scholarpedia **9**(6): 9806, (2014).
- [2] G. E. Mitchell, A. Richter, and H. A. Weidenmüller: *Random Matrices and Chaos in Nuclear Physics: Nuclear Reactions*, Rev. Mod. Phys. **82** (2010), 2845–2901.
- [3] H.-J. Stöckmann: *Quantum Chaos: An Introduction*, (Cambridge University Press, Cambridge), (1999).
- [4] G. Tanner and N. Søndergaard: *Wave Chaos in Acoustics and Elasticity*, J. Phys. A **40** (2007), R443–R509.
- [5] R. A. Jalabert: *Mesoscopic Transport and Quantum Chaos*, Scholarpedia **11**(1): 30946, (2016).
- [6] H. Cao and J. Wiersig: *Dielectric microcavities: Model systems for wave chaos and non-Hermitian physics*, Rev. Mod. Phys. **87** (2015), 61–111.
- [7] A. Voros: *Semi-classical ergodicity of quantum eigenstates in the Wigner representation*, in: *Stochastic Behavior in Classical and Quantum Hamiltonian Systems* (Eds. G. Casati and J. Ford), vol. 93 of *Lecture Notes in Physics*, 326–333, (Springer Berlin Heidelberg, Berlin), (1979).
- [8] M. V. Berry: *Regular and irregular semiclassical wavefunctions*, J. Phys. A **10** (1977), 2083–2091.
- [9] M. V. Berry: *Semiclassical mechanics of regular and irregular motion*, in: *Comportement Chaotique des Systèmes Déterministes — Chaotic Behaviour of Deterministic Systems* (Eds. G. Iooss, R. H. G. Helleman and R. Stora), 171–271, (North-Holland, Amsterdam), (1983).
- [10] A. I. Shnirelman: *Ergodic properties of eigenfunctions* (in Russian), Usp. Math. Nauk **29** (1974), 181–182.
- [11] Y. Colin de Verdière: *Ergodicité et fonctions propres du laplacien* (in French), Commun. Math. Phys. **102** (1985), 497–502.
- [12] S. Zelditch: *Uniform distribution of eigenfunctions on compact hyperbolic surfaces*, Duke. Math. J. **55** (1987), 919–941.
- [13] S. Zelditch and M. Zworski: *Ergodicity of eigenfunctions for ergodic billiards*, Commun. Math. Phys. **175** (1996), 673–682.
- [14] S. De Bièvre: *Quantum chaos: a brief first visit*, in: *Second Summer School in Analysis and Mathematical Physics (Cuernavaca, 2000)* (Eds. S. Pérez-Esteve and C. Villegas-Blas), Contemp. Math. **289**, 161–218. Amer. Math. Soc., Providence, RI, (2001).
- [15] S. Nonnenmacher and A. Voros: *Chaotic Eigenfunctions in Phase Space*, J. Stat. Phys. **92** (1998), 431–518.
- [16] A. Bäcker, R. Schubert, and P. Stifter: *Rate of quantum ergodicity in Euclidean billiards*, Phys. Rev. E **57** (1998), 5425–5447, ; erratum *ibid.* **58** (1998) 5192.
- [17] H. Ishio, A. I. Saichev, A. F. Sadreev, and K.-F. Berggren: *Wave Function Statistics for Ballistic Quantum Transport through Chaotic Open Billiards: Statistical Crossover and Coexistence of Regular and Chaotic Waves*, Phys. Rev. E **64** (2001), 056208.
- [18] Y.-H. Kim, M. Barth, H.-J. Stöckmann, and J. P. Bird: *Wave Function Scarring in Open Quantum Dots: A Microwave-Billiard Analog Study*, Phys. Rev. B **65** (2002), 165317.
- [19] A. Bäcker, A. Manze, B. Huckestein, and R. Ketzmerick: *Isolated resonances in conductance fluctuations and hierarchical states*, Phys. Rev. E **66** (2002), 016211.
- [20] B. Weingartner, S. Rotter, and J. Burgdörfer: *Simulation of Electron Transport through a Quantum Dot with Soft Walls*, Phys. Rev. B **72** (2005), 115342.
- [21] T. Weich, S. Barkhofen, U. Kuhl, C. Poli, and H. Schomerus: *Formation and interaction of resonance chains in the open three-disk system*, New J. Phys. **16** (2014), 033029.
- [22] C. Gmachl, F. Capasso, E. E. Narimanov, J. U. Nöckel, A. D. Stone, J. Faist, D. L. Sivco, and A. Y. Cho: *High-Power Directional Emission from Microlasers with Chaotic Resonators*, Science **280** (1998), 1556–1564.
- [23] S.-Y. Lee, S. Rim, J.-W. Ryu, T.-Y. Kwon, M. Choi, and C.-M. Kim: *Quasiscattered Resonances in a Spiral-Shaped Microcavity*, Phys. Rev. Lett. **93** (2004), 164102.
- [24] J. Wiersig and M. Hentschel: *Combining Directional Light Output and Ultralow Loss in Deformed Microdisks*, Phys. Rev. Lett. **100** (2008), 033901.
- [25] S. Shinohara, T. Harayama, T. Fukushima, M. Hentschel, T. Sasaki, and E. E. Narimanov: *Chaos-Assisted Directional Light Emission from Microcavity Lasers*, Phys. Rev. Lett. **104** (2010), 163902.
- [26] J.-B. Shim, J. Wiersig, and H. Cao: *Whispering gallery modes formed by partial barriers in ultrasmall deformed microdisks*, Phys. Rev. E **84** (2011), 035202.
- [27] T. Harayama and S. Shinohara: *Ray-Wave Correspondence in Chaotic Dielectric Billiards*, Phys. Rev. E **92** (2015), 042916.
- [28] G. Casati, G. Maspero, and D. L. Shepelyansky: *Quantum fractal eigenstates*, Physica D **131** (1999), 311–316.
- [29] H. Schomerus and J. Tworzydło: *Quantum-to-Classical Crossover of Quasibound States in Open Quantum Systems*, Phys. Rev. Lett. **93** (2004), 154102.
- [30] J. P. Keating, M. Novaes, S. D. Prado, and M. Sieber: *Semiclassical Structure of Chaotic Resonance Eigenfunctions*, Phys. Rev. Lett. **97** (2006), 150406.
- [31] S. Nonnenmacher and M. Rubin: *Resonant eigenstates for a quantized chaotic system*, Nonlinearity **20** (2007), 1387.
- [32] L. Ermann, G. G. Carlo, and M. Saraceno: *Localization of Resonance Eigenfunctions on Quantum Repellers*, Phys. Rev. Lett. **103** (2009), 054102.
- [33] G. G. Carlo, D. A. Wisniacki, L. Ermann, R. M. Benito, and F. Borondo: *Classical transients and the support of open quantum maps*, Phys. Rev. E **87** (2013), 012909.
- [34] M. Schönwetter and E. G. Altmann: *Quantum signatures of classical multifractal measures*, Phys. Rev. E **91** (2015), 012919.
- [35] M. J. Körber, A. Bäcker, and R. Ketzmerick: *Localization of Chaotic Resonance States due to a Partial Transport Barrier*, Phys. Rev. Lett. **115** (2015), 254101.
- [36] S. Fishman: *Anderson Localization and Quantum Chaos Maps*, Scholarpedia **5**(8): 9816, (2010).
- [37] E. J. Heller: *Bound-State Eigenfunctions of Classically Chaotic Hamiltonian Systems: Scars of Periodic Orbits*, Phys. Rev. Lett. **53** (1984), 1515–1518.
- [38] Y.-C. Lai and T. Tél: *Transient Chaos: Complex Dynamics on Finite Time Scales*, no. 173 in Applied Mathematical Sciences, (Springer Verlag, New York), 1st edn., (2011).
- [39] G. Pianigiani and J. A. Yorke: *Expanding Maps on Sets Which Are Almost Invariant: Decay and Chaos*, Trans. Amer. Math. Soc. **252** (1979), 351–366.
- [40] H. Kantz and P. Grassberger: *Repellers, semi-attractors, and long-lived chaotic transients*, Physica D **17** (1985),

- 75–86.
- [41] T. Tél: *Escape rate from strange sets as an eigenvalue*, Phys. Rev. A **36** (1987), 1502–1505.
- [42] A. Lopes and R. Markarian: *Open Billiards: Invariant and Conditionally Invariant Probabilities on Cantor Sets*, SIAM J. Appl. Math. **56** (1996), 651–680.
- [43] M. F. Demers and L.-S. Young: *Escape rates and conditionally invariant measures*, Nonlinearity **19** (2006), 377–397.
- [44] E. G. Altmann, J. S. E. Portela, and T. Tél: *Leaking chaotic systems*, Rev. Mod. Phys. **85** (2013), 869–918.
- [45] M. Novaes: *Supersharp resonances in chaotic wave scattering*, Phys. Rev. E **85** (2012), 036202.
- [46] B. V. Chirikov: *A universal instability of many-dimensional oscillator systems*, Phys. Rep. **52** (1979), 263–379.
- [47] M. V. Berry, N. L. Balazs, M. Tabor, and A. Voros: *Quantum maps*, Ann. Phys. (N.Y.) **122** (1979), 26–63.
- [48] S.-J. Chang and K.-J. Shi: *Evolution and exact eigenstates of a resonant quantum system*, Phys. Rev. A **34** (1986), 7–22.
- [49] F. Borgonovi, I. Guarneri, and D. L. Shepelyansky: *Statistics of Quantum Lifetimes in a Classically Chaotic System*, Phys. Rev. A **43** (1991), 4517–4520.